Electronic Structure of 3,7-Diphenyl- and 3,7-Bis(dimethylamino)-1,5-dithia-2,4,6,8-tetrazocines: Ab Initio Calculations and Photoelectron Spectra

J. P. Boutique,*[†,‡] J. Riga,[†] J. J. Verbist,[†] J. Delhalle,[§] J. G. Fripiat,[§] R. C. Haddon,[⊥] and M. L. Kaplan[⊥]

Contribution from the Laboratoire de Spectroscopie Electronique, Facultes Universitaires Notre-Dame de la Paix, B-5000 Namur, Belgium, Laboratoire de Chimie Theorique Appliquee, Facultes Universitaires Notre-Dame de la Paix, B-5000 Namur, Belgium, and AT&T Bell Laboratories, Murray Hill, New Jersey 07974. *Received June 13, 1983*

Abstract: The 8-membered ring system, 1,5-dithia-2,4,6,8-tetrazocine, consists of two -NSN- units joined by carbon atoms. With phenyl groups substituted on the carbon atoms, the hetero ring is coplanar. Replacement of the phenyl groups with electron-donating substituents such as dimethylamino leads to a bent ring configuration with strong cross-ring sulfur-sulfur interactions. This behavior has been subjected to both experimental and theoretical examination. Electronic structure and ground-state properties of the structurally different 3,7 diphenyl- and 3,7-bis(dimethylamino)-1,5-dithia-2,4,6,8-tetrazocines are studied by STO-3G (+5D) ab initio calculations and X-ray photoelectron spectroscopy. The agreement reached between theory and experiment (core level shifts and the shape of valence bands) allows the proposal of a detailed interpretation of the structural behavior of the $S_2N_4C_2$ heterocycle.

The preparation of $(SN)_x$ and $(CH)_x$ conducting polymers has stimulated efforts toward the synthesis of related macromolecules such as $(SCH)_x$ and $(C(R)NSN)_x$, which could exhibit similar and hopefully better conducting properties. In spite of the inconclusive nature of these attempts, new molecules with uncommon structures and interesting properties have emerged.

Among these compounds, the 3,7-diphenyl- and 3,7-bis(dimethylamino)-1,5-dithia-2,4,6,8-tetrazocines, referred to as DTZ and DIATZ, display the novel 1,5-dithia-2,4,6,8-tetrazocine ring structure, $S_2N_4C_2$[1] (Figure 1) and add to the family of systems with similar rings such as $S_2N_4As_2$ and $S_2N_4Si_2$, already reported in the literature,[2-5] which are all related to tetrasulfur tetranitride, S_4N_4, the precursor of $(SN)_x$.[6]

As indicated by X-ray diffraction measurements,[1] the DTZ and DIATZ geometries are quite different (Figure 1). In DTZ, the dithiatetrazocine ring is perfectly planar, with only the phenyl groups twisted out of the $S_2N_4C_2$ plane (at an angle of 9.7°). In contrast, DIATZ is folded along an axis passing through the two sulfur atoms with a dihedral angle of 101°, and except for the methyl hydrogens, all atoms lie in two planes intersecting this axis. Geometric parameters[1] are given in Figure 1.

Except for electronic delocalization schemes[1] conjectured from the above-mentioned structural evidence, a more comprehensive interpretation of the DTZ and DIATZ structural behavior is still missing. Using ab initio quantum mechanical calculations, we obtained a description of the DTZ and DIATZ electronic structure, generally confirmed by original X-ray photoelectron spectroscopy data, and therefore propose a theoretically grounded interpretation of the behavior of these systems.

Experimental Section

XPS Measurements. The compounds, prepared according to the methods originally reported in the literature,[1] were crushed and pressed in pellet form on a gold substrate. XPS spectra were recorded at room temperature on a Hewlett-packard 5950A spectrometer using the Al $K\alpha_{1,2}$ monochromatized radiation ($h\nu$ = 1486.6 eV) as the incident photon source. The pressure was kept in the range of $2-4 \times 10^{-9}$ torr during data acquisitions. The flood-gun technique had to be used to neutralize the buildup of positive charges on the sample surface. Even after long accumulation periods, the compounds remained totally free of oxygen contamination as verified by the absence of the O1s peak in the spectra.

Due to the phenyl group contained in DTZ, it was possible to assign directly their C1s peaks by comparison to the 284.4-eV binding energy found in graphite.[7] Unfortunately the same procedure is inapplicable to DIATZ and the calibration was made by following an established procedure.[8] With polyethylene added to the sample, the C1s binding energy of polyethylene at 284.6 eV was used for calibration by reference to the $Au4F_{7/2}$ level (84.0 eV).

All experimental spectra given hereafter are direct recordings, except for valence bands which were smoothed by a second degree polynomial least square fitted to nine experimental points at a time. Since these experimental valence spectra had to be compared with corresponding theoretical simulations, it was necessary to subtract from the former a sigmoid background whose amplitude at a given kinetic energy is proportional to the fraction of electrons with a larger kinetic energy.

Theoretical Methodolgy. Restricted Hartree-Fock-Roothaan (LCAO-MO-SCF) results on DTZ and DIATZ have been obtained with STO-3G and STO-3G+5D basis sets by using the GAUSSIAN 80 program.[9] Geometries used in these calculations are slight modifications of the experimental ones[1] to accommodate D_{2h} and C_{2v} point group symmetries for DTZ and DIATZ, respectively. All integrals larger than 10^{-6} were explicitly taken into account and the convergence threshold on the density matrix elements was 5×10^{-5}. STO-3G and STO-3G+5D (five d atomic functions contracted from six Cartesian Gaussians) basis sets are directly taken from the work of Pople and co-workers[10] on third row atoms. In spite of limitations inherent to restricted basis sets, we have used them to compute (1) electron charges on atoms and Mulliken overlap populations to characterize the bonding, (2) total energies to differentiate semiquantitatively between two conformations of DIATZ,

[†] Laboratoire de Spectroscopie Electronique.
[§] Laboratoire de Chimie Theorique Appliquee.
[‡] Holder of an I.R.S.I.A. fellowship and presently Research Assistant of the F.N.R.S. (Belgium).
[⊥] AT&T Bell Laboratories.

(1) Ernest, I.; Hollick, W.; Rihs, G.; Schomburg, D.; Shoham, G.; Wenkert, D.; Woodward, R. B. *J. Am. Chem. Soc.* **1981**, *103*, 1540.
(2) Scherer, O. J.; Wies, R., *Angew. Chem., Int. Ed. Engl.* **1971**, *10*, 812.
(3) Alcock, N. W.; Holt, E. M.; Kuyper, J.; Mayerle, J. J.; Street, G. D. *Inorg. Chem.* **1979**, *18*, 2235.
(4) (a) Roesky, H. W.; Wiezer, H., *Chem. Ztg.* **1973**, *97*, 661. (b) Ertl, G.; Weiss, J. *Z. Naturforsch. B* **1974**, *29B*, 803.
(5) Gleiter, R., *Angew. Chem., Int. Ed. Engl.* **1981**, *20*, 444.
(6) (a) Lu, G. S.; Donohue, J. *J. Am. Chem. Soc.* **1944**, *66*, 818. (b) Clark, D.; *J. Chem. Soc.* **1952**, *1615*. (c) Sharma, B. D.; Donohue, J. *Acta Crystallogr.* **1963**, *16*, 891.
(7) Werthelm, G. K.; Van Attekum, P.M.T.M.; Basu, S. *Solid State Commun.* **1980**, *33*, 1127.
(8) Boutique, J. P.; Riga, J.; Verbist, J. J.; Delhalle, J.; Friplat, J. G.; Andre, J. M.; Haddon, R. C.; Kaplan, M. L. *J. Am. Chem. Soc.* **1982**, *104*, 2691.
(9) Binkley, J. S.; Whiteside, R. A.; Raghavachari, K.; Seeger R.; Defrees, D. J.; Schlegel, H. B.; Topiol, S.; Kahn, L. R.; Pople, J. A., *QCPE* **1981**, *13*, 406.
(10) (a) Hehre, W. J.; Ditchfield, R.; Stewart, R. F.; Pople, J. A. *J. Chem. Phys.* **1970**, *52*, 2769. (b) Collins, J. B.; Schleyer, P. v. R.; Binkley, J. S.; Pople, J. A. *J. Chem. Phys.* **1976**, *64*, 5142.

0002-7863/84/1506-0312$01.50/0

Table I. Results of Theoretical Calculations on DTZ, DIATZ and DIATZP

	DTZ		DIATZ		DIATZP
	STO-3G	STO-3G+5D	STO-3G	STO-3G+5D	STO-3G
			Total Energy (au)		
	−1530.51661	−1530.82225	−1339.96517	−1340.24443	−1339.92388
			Electronic Charges		
S_1	15.334	15.653	15.391	15.636	15.346
N_2	7.448	7.293	7.500	7.391	7.480
C_3	5.812	5.803	5.670	5.641	5.694
C_4, N_4	5.995	5.991	7.277	7.275	7.288
C_5	6.059	6.059			
C_6	6.064	6.066			
C_7	6.064	6.065			
			Mulliken Overlap Populations		
$3p_x$-$3p_x$:S_1-S'	0.001	0.001	0.077	0.092	0.0
$3p_z$-$2p_z$:S_1-N_2	0.056	0.060	*a*	*a*	0.051
$2p_z$-$2p_z$:N_2-C_3	0.104	0.098	0.092	0.085	0.100
C_3-C_4, C_3-N_4	0.018	0.021	0.061	0.066	0.038
C_4-C_5, N_4-C_5	0.106	0.105			0.004
C_5-C_6	0.110	0.110			
[b] $3d_{yz}$-$2p_z$:S_1-N_2		0.042		*a*	

[a] Meaningless. [b] All the other overlap populations involving S3d orbitals are negligible.

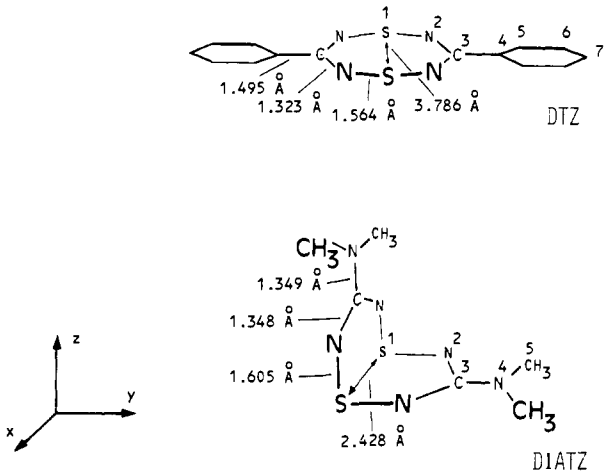

Figure 1. Schematic molecular structures of DTZ and DIATZ.

and (3) one-electron energies to interpret XPS core and valence spectra of both DTZ and DIATZ. This approach has proved its usefulness and reliability in studies on related compounds.[8,11]

Correlations of the spectral and calculated data are based on the assumed validity of Koopmans' theorem. Our interpretative support is significantly enhanced by comparing measured spectra and corresponding simulations constructed from theoretical results. The calculations of the simulated spectra rest on the Gelius intensity model[12] where the intensity of the jth one-electron state, I_j, is a weighted sum of products of net atomic populations, $P_{A\lambda_j}$, with the corresponding atomic function (AO) relative cross section

$$I_j = \left(2 + \frac{\beta}{2}\right) \sum_{A,\lambda} P_{A\lambda_j} \frac{\sigma_{A\lambda}^{AO}}{\sigma_{A\phi\lambda_0}^{AO}}$$

where λ is the angular momentum quantum number of atomic orbital A and β is an asymmetry parameter of molecular orbital j. For each moleculare orbital, the sum is extended over all valence atomic orbitals. In the calculations of the simulated spectra, only the STO-3G basis was used and the β asymmetry parameter was arbitrarily set to 2 for each molecular orbital. The theoretical spectra are constructed from a series of peaks located at each one-electron eigenvalue, ϵ_j, on the energy scale, and linearly contracted in energy to obtain the best overall fit with the experimental spectrum. The final shape is then obtained from a combination of one Lorentzian and one Gaussian centered on the ϵ_j's, with each having the same intensity and width (1.5 eV) over the energy range.

Calculations reported in this work were carried out on the DEC 2060 computer of the Facultes Universitaires Computing Center.

Theoretical Results

In this section, we first inspect the theoretical electron distributions of DTZ and DIATZ molecules through the Mulliken population analysis, and therefrom determine the bonding character of the one-electron levels to be correlated with XPS spectra in the next section. To help in comprehending the origin of the marked structural differences exhibited by DTZ and DIATZ molecules, we have also considered a hypothetical planar form of DIATZ, DIATZP, obtained by replacing the phenyl substituents on the DTZ-$S_2N_4C_2$ ring by two dimethylamino groups linked with the same C_3–N_4 distance (1.343 Å) as in the normal DIATZ. Table I compares the calculated total energies, gross atomic charges, and selected overlap populations of these molecules.

Total energies in both STO-3G and STO-3G+5D basis sets are reported here for indicative purposes; extension of the STO-3G basis set by including d functions on sulfur atoms yields, as expected, slightly lower energy values. Though no geometry optimization was actually conducted, the 25.9 kcal mol^{-1} energy difference (STO-3G) between DIATZ and DIATZP points to a strong stabilization upon folding the $S_2N_4C_2$ cycle, which cannot be explained solely by crystal packing effects.

These calculations show that the dithiatetrazocine ring is formed of positively charged sulfur and carbon atoms alternating with negative nitrogens. However, the amount of charge separation in DTZ and DIATZ is smaller than that formed in the S_4N_4 cycle.[13,14] The π overlap populations relative to the S_1–N_2 and N_2–C_3 bonds have values that approach that expected for partial double bond character. Introduction of d atomic functions on sulfur atoms reduces the polarity of the S–N bond,[14] but these extra functions do not play an important part in the bond formation between the two sulfur atoms in DIATZ.

Calculated atomic charges indicate an electron migration from C_3 to N_2 as the phenyl substituents are replaced by dimethylamino groups. In both DTZ and DIATZ, the charges on the sulfur atoms are nearly equal. This somewhat unexpected observation, in view of the different conformations, is experimentally confirmed by the S2P core level analysis (vide infra). Notice also the somewhat larger electron redistribution in DIATZ with a twisted eight-membered ring, compared to DIATZP where the cycle is forced to be planar.

(11) Findlay, R. H.; Palmer, H. H.; Downs, A. J.; Egdel, R. G.; Evans, R. *Inorg. Chem.* **1980**, *19*, 1307.

(12) (a) Gelius, U. "Electron Spectroscopy"; Shirley, D. A., Ed.; North-Holland: Amsterdam, 1972; p 311. (b) Gelius, U. *J. Electron Spectrosc. Relat. Phenom.* **1974**, *5*, 985.

(13) Milleflori, A.; Milleflori, S. *J. Chem. Res., Synop.* **1980**, 244.

(14) Haddon, R. C.; Wasserman, S. R.; Wudl, F.; Williams, G. R. J. *J. Am. Chem. Soc.* **1980**, *102*, 6687.

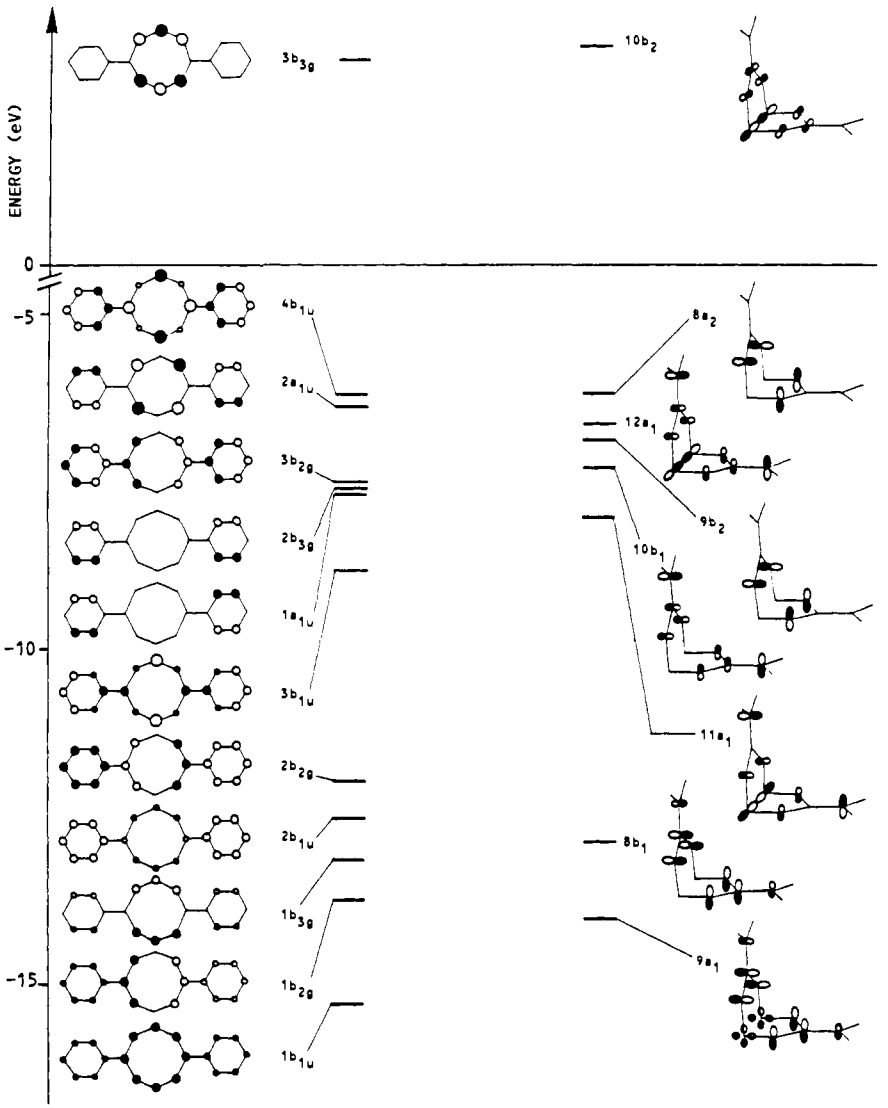

Figure 2. Comparison of the "π" electronic levels of DTZ and DIATZ.

Two essential points should be underscored with regard to the overlap population data. First, the $S3p_x$–$S3p_x$ overlap population, nearly zero in DTZ, has a much larger value in DIATZ corresponding to the long (2.428 Å) sulfur–sulfur transannular interaction similar to that present in S_4N_4 (2.56 Å).[5,6,15] Second, the large differences between C_32p_z–C_42p_z (DTZ) and C_32p_z–N_42p_z (DIATZ) overlap populations illustrate the essential role played by the substitutents on the $S_2N_4C_2$ electronic and geometric structure. This is further evidenced by the values assumed by the C_32p_z–N_42p_z overlap population in DIATZ (0.061) and DIATZP (0.038), which is in apposition to the idea that a charge flow from the $N(CH_3)_2$ groups should be easier within a fully conjugated structure.

These data substantiate the schematic pictures of electron delocalization in DTZ and DIATZ proposed by Ernest et al. (Figures 3a and 4a in ref 1). The replacement of the phenyl units by the mesomeric electron donor groups, $N(CH_3)_2$, induces an electronic charge transfer into the $S_2N_4C_2$ ring, thereby causing the endocyclic nitrogen atoms to become more negative. Part of this charge transfer is used to form a "long" S–S bond, thus forcing the ring structure to adjust to a bicyclic conformation. Indeed, a planar situation would be energetically unfavorable, due to the difficulty in maintaining "three" bonds from the sulfur atoms in an angular sector smaller than 180°. A more stable geometry is then obtained through the already mentioned distortion of the $S_2N_4C_2$ ring and results in a partial loss of symmetry.

(15) Gleiter, R. *J. Chem. Soc. A* **1970**, *3174*.

The observed structures of DTZ and DIATZ are well rationalized by the $4n + 2$ Hückel rule. Formally, the dithiatetrazocine ring contains 10 π electrons ($C2p^1$; $N2p^1$; $S3p^2$), and, according to this $4n + 2$ rule, the $S_2N_4C_2$ cycle should be aromatic and planar as is the case for DTZ. However, due to the electronic perturbation in DIATZ, the conditions for the $4n + 2$ rule are no longer met, leading to a reduction in aromaticity and electron delocalization. This can be related to the case of S_4N_4 and $S_4N_4^{2+}$. The dication, $S_4N_4^{2+}$, contains 10 π electrons, and indeed is found to be planar,[15] while S_4N_4 with its additional 2 electrons in the π system adopts a cradle-like structure.[6c]

The dithiatetrazocine cycle is likely to be aromatic and planar in those compounds where substituents on the ring carbons contribute to an appropriate mesomeric effect. This seems essential in view of the difficulties encountered in synthesizing[1] the $S_2N_4C_2H_2$ system. The hydrogen and carbon electronegativities are comparable, and inductive charge transfer should be minor, thus leaving the $4n + 2$ rule approximately fulfilled. The fact that $S_2N_4C_2H_2$ has not been synthesized tends to indicate that some sort of mesomeric stabilization is also needed from the substituents.

For DTZ and DIATZ respectively, Tables II and III give the one-electron enegies, the point group irreducible representation lables of the one-electron states (MO), the the dominant atomic functions entering into their expressions. Except for the lowest unoccupied molecular orbital (LUMO) in DIATZ, only the π-type MO's are considered in Figure 2 where STO-3G one-electron levels of both compounds are schematically contrasted. Due to the nonplanarity of DIATZ, one cannot, strictly speaking, use a "π-

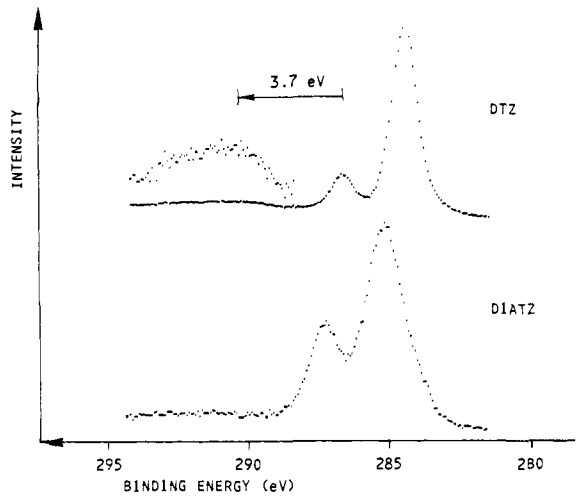

Figure 3. X-ray photoelectron spectra of the C1s levels of DTZ and DIATZ.

type" nomenclature to characterize the molecular orbitals. However, in analogy with DTZ and to facilitate the comparison, we purposely use this terminology on the half of the DIATZ placed in the same orientation as DTZ (see also Figure 1).

In both molecules, the three highest occupied MO's are of "π-type". They are followed, at lower energy, by MO's characteristic of the phenyl ($2b_{3g}$ and $1a_{1u}$ in DTZ) and the dimethylamino ($10b_1$ and $7a_2$ in DIATZ) substituent groups which appear in the 7–8-eV energy range. Invoking well-known relationships between the HOMO and the molecular ground-state properties of π-systems,[16] it is possible to rationalize some of the features of DTZ and DIATZ. In DTZ, the HOMO exhibits maxima on the sulfur and endocyclic carbon atoms, and minima on nitrogens; it belongs to the b_{1u} irreducible representation of the D_{2h} point group. In the HOMO of DIATZ, the electron density is predominantly located on the four nitrogens of the cycle and vanishingly small on the other atoms of the cycle. It is interesting to observe that the HOMO in DIATZ corresponds to the penultimate ($2a_{1u}$) occupied orbital in DTZ. The energy of the former is higher largely due to the breakdown of planarity. In spite of their different nature, the HOMO's of both compounds are very close to each other on the energy scale. Adding d functions of the sulfur does not change this picture.

The nature of the LUMO in DTZ is very informative on the structural evolution from DTZ to DIATZ. The LUMO describes a strong antibonding interaction between endocyclic sulfur and nitrogen atoms. Enhancing the electron density on the dithiatetrazocine cycle, in other words populating the LUMO, induces a destabilization in the heterocycle. Such a result is experimentally observed in DIATZ.

Before entering the next section, where experimental results will be compared with the calculated one-electron states, it is worth recalling the limited nature of the basis set used. More extended bases, which we did not apply, could possibly induce slight modifications in the distribution of the one-electron energies. However, no change in the qualitative picture presented here is to be expected.

Experimental Results

We will now analyze in detail the XPS data obtained for DTZ and DIATZ.

A. Core Levels. The essential characteristics of the core levels are given in Table IV. The DTZ C1s line shows two components with a 1:6 intensity ratio (Figure 3), in good agreement with the calculated charges. We attribute the high binding energy peak to the positively charged endocyclic carbons. A broad structure composed of several satellite lines is observed at 290.3 eV. Again

(16) Gillespie, R. J.; Kent, J. P.; Sawyer; J. F.; Slim, D. R.; Tyrer, J. D.; *Inorg. Chem.* **1981**, 20, 3799.

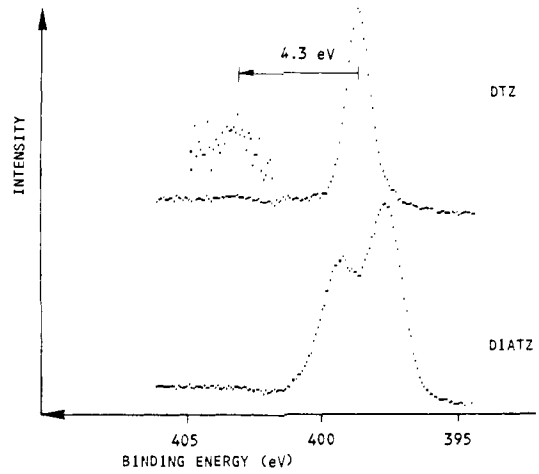

Figure 4. X-ray photoelectron spectra of the N1s levels of DTZ and DIATZ.

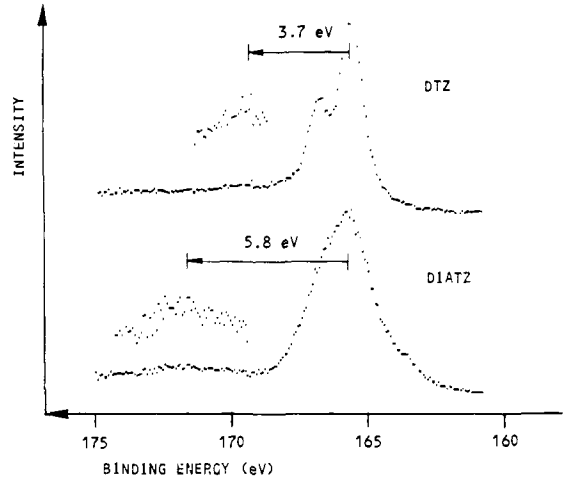

Figure 5. X-ray photoelectron spectra of the S2p levels of DTZ and DIATZ.

the observed binding energies confirm the theoretical results of Table I, where the DIATZ endocyclic carbons (E_b = 287.3 eV) are more positive than in DTZ (E_b = 286.6 eV, Figure 3). However, the expected 1:2 intensity ratio between the C1s lines in DIATZ is not observed. This discrepancy very likely has its origin in an impurity associated with the shoulder on the right hand side of the main C1s peak (~284.0 eV).

The chemical shift to lower binding energies observed on the endocyclic N1s lines (Table IV, Figure 4) supports the calculated negative charges, while the N1s peak attributed to the nitrogen of the amion groups is found at 399.4 eV, an energy value typical of a neutral nitrogen.[17] A satellite structure is also present at 403.0 eV in the N1s spectrum of DTZ (Figure 4).

The S2p lines of both compounds (Figure 5) appear at a relatively high binding energy, compatible with the predicted sulfur gross atomic charges in Table I. A satellite is found at 169.1 eV for DTZ and 171.3 eV for DIATZ. The shape of the S2p doublet is less resolved in the case of DIATZ. This is attributed to the presence of an impurity around 164 eV and is tentatively interpreted as residual elemental sulfur which is a byproduct of the preparation rection.[1]

B. Valence Levels. The smoothed experimental and theoretically simulated valence XPS spectra are shown in Figure 6; their essential features are summarized in Table V.

(17) (a) Stretlwieser, A.; Jr., "Molecular Orbital Theory for Organic Chemists"; Wiley: New York, 1961. (b) Salem, L. "The Molecular Orbital Theory of Conjugated Systems"; W. A. Benjamin: New York, 1966. (c) Dewar, M. J. S. "The Molecular Orbital Theory of Organic Chemistry"; McGraw-Hill: New York, 1969.

Table II. One-Electron Levels of DTZ (eV)

label	energy (no. of levels) STO-3G	STO-3G+5D	assignment	intensity
S1s	−2475.56 (2)	−2465.52 (2)	S	
N1s	416.53 (4)	417.68 (4)	N	
C1s	302.78 (2)	303.07 (2)	C_3	
	300.37 (2)	300.44 (2)	C_4	
	300.05 (2)	300.14 (2)	C_2	
	300.01 (8)	300.09 (8)	C_5, C_6	
S2s	240.96 (2)	240.39 (2)	S	
S2p	176.55 (2)	176.98 (2)		
	176.43 (2)	176.90 (2)		
	176.43 (2)	176.89 (2)		
$1a_{1g}$	34.64	34.23	N2s, S3s	1084
$1b_{3u}$	32.89	32.95	N2s, S3s	1280
$1b_{2u}$	32.82	32.19	N2s, S3s	1089
$2a_{1g}$	29.89	29.93	C2s	835
$2b_{3u}$	29.73	29.80	C2s	862
$1b_{1g}$	29.57	29.69	N2s	1567
$3a_{1g}$	27.56	27.38	S3s, N2s	824
$3b_{3u}$	26.29	26.37	C2s	976
$2b_{2u}$	25.99	26.06	C2s	932
$2b_{1g}$	25.95	26.02	C2s	947
$4a_{1g}$	25.32	25.23	S3a, C2s	919
$3b_{2u}$	22.94	22.90	S3s, N2s, C2s	870
$4b_{3u}$	22.51	22.59	N2s,2p, C2s	865
$3b_{1g}$	20.99	21.09	C2s,2p	674
$5a_{1g}$	20.86	20.90	S3s, C2s,2p	718
$4b_{2u}$	20.66	20.73	S3s, C2s,2p	781
$5b_{3u}$	20.19	20.23	C2s, S3p, N2p	666
$4b_{1g}$	18.32	18.45	N2p, S3p, C2p	265
$6a_{1g}$	18.29	18.36	C2p	138
$6b_{3u}$	18.04	18.10	C2p	93
$7s_{1q}$	16.47	16.54	C2s, S3a	590
$7b_{3u}$	16.15	16.21	C2s,2p	565
$8a_{1g}$	15.33	15.41	S3p, N2p, C2s,2p	329
$1b_{1u}$	15.27	15.14	π	299
$5b_{2u}$	15.15	15.21	C2p	173
$8b_{3u}$	15.00	15.06	C2p	184
$5b_{1g}$	14.95	15.03	C2p	120
$6b_{2u}$	14.50	14.57	C2p	128
$6b_{1g}$	14.46	14.54	C2p	110
$1b_{2g}$	13.70	13.83	π	121
$7b_{2u}$	13.31	13.18	S3p, N2p	566
$1b_{3g}$	13.13	12.70	π	568
$9a_{1g}$	12.80	12.90	S3p, N2p	518
$2b_{1u}$	17.49	12.52	π	141
$10a_{1g}$	12.11	12.29	S3s, N2s,2p	1761
$9b_{3u}$	12.04	12.12	C2p	143
$2b_{2g}$	11.95	12.06	π	121
$8b_{2u}$	11.79	11.87	C2p	128
$7b_{1g}$	11.73	11.81	C2p	95
$11a_{1g}$	11.10	11.04	S3p	612
$9b_{2u}$	8.98	9.47	N2p, S3s,3p	1196
$3b_{1u}$	8.82	8.60	π	352
$10b_{3u}$	8.70	9.03	N2p, S3p	780
$8b_{1g}$	8.27	8.59	N2p	292
$1a_{1u}$	7.56	7.64	π	131
$2b_{3g}$	7.56	7.63	π	131
$3b_{2g}$	7.50	7.62	π	138
$2a_{1u}$	6.36	7.30	π	221
$4b_{1u}$ (HOMO)	−6.18	−5.71	π	403
$3b_{3g}$ (LUMO)	+3.12	+3.64	π	

In the DTZ spectrum, peaks A and B result from molecular orbitals having a strong N2s character, whereas peaks C and D are related to σ N2s–C2s and N2s–S3s interactions. Structure E is due to the $7b_{3u}$ and $7a_{1g}$ levels that describe the C2s–C2s interactions. The major part of peaks F and G is due to the presence of the intense σ $10a_{1g}$ and $9b_{2u}$ (N2p–S3p) contributions. From the calculated intensity values, the HOMO of DTZ (π $4b_{1u}$) is predicted to be more intense than the neighboring occupied MO; thus the HOMO determines the centroid of structure H.

The agreement between the experimental and simulated spectra is generally satisfactory, except for the valley between the G and H peaks (DTZ), which is hardly visible in the simulated spectrum. We relate this deficiency to the 1.5-eV width imposed for each MO in the convolution. This value is probably too large to adequately reproduce the XPS lone pair peaks.

The XPS valence band spectrum of DIATZ looks very different, particularly in the 4-eV binding energy region. Moreover, the agreement between experimental and simulated spectra is considerably poorer. We think that these discrepancies find their origin in the impurities already mentioned in the context of the core level analysis. The lack of experimentally well-resolved structures in the range from peak D to G would be related to the presence of additional valence levels, originating from elemental sulfur and other uncharacterized secondary products.

The G peak should not be confused with the HOMO. As a matter of fact, the HOMO is predited to appear at nearly the same

Table III

label	energy (no. of levels) STO-3G	STO-3G+5D	assignment	intensity
S1s	−2475.31 (2)	−2475.51 (2)	S	
N1s	417.96 (2)	418.12 (2)	N_4	
	414.44 (4)	414.82 (4)	N_2	
C1s	303.72 (2)	303.97 (2)	C_3	
	301.56 (4)	301.68 (4)	C_5	
S2s	240.76 (2)	240.39 (2)	S	
S2p	176.32 (2)	176.11 (2)		
	176.28 (2)	175.96 (2)		
	176.26 (2)	175.81 (2)		
$1a_1$	35.10	34.55	S3s, N2s, C2s	965
$1b_1$	33.67	33.67	N2s, C2s	1194
$2a_1$	32.13	31.94	N2s	1140
$1b_2$	31.65	30.89	S3s, N2s	1100
$2b_1$	30.46	30.25	N2s	1281
$1a_2$	28.11	27.89	N2s	1510
$3a_1$	26.00	25.70	S3s, C2s	918
$2b_2$	25.29	25.35	N2p, C2s	818
$2a_2$	25.09	25.14	N2p, C2s	903
$3b_1$	23.86	23.89	C2s, N2p	873
$4a_1$	22.38	22.18	S3s, N2p	1045
$3b_2$	21.55	21.25	S3s	975
$4b_1$	18.79	18.78	S3p, C2p	837
$5a_1$	17.71	17.66	S3s, N2s	673
$6a_1$	17.28	17.05	S3p, N2s,2p	603
$3a_2$	16.86	16.84	S3p, C2p	250
$7a_1$	16.63	16.61	S3p, C2p, H1s	204
$5b_1$	16.61	16.64	C2p, N2p	94
$6b_1$	16.36	16.27	S3p, C2s, C2p	361
$4b_2$	15.34	15.35	S3s, N2p, C2p	329
$4a_2$	14.49	14.55	C2p, H1s	61
$5b_2$	14.48	14.54	C2p, H1s	56
$8a_1$	14.38	14.38	S3p, C2p, H1s	282
$5a_2$	14.29	14.31	S3p, N2p, C2p, H1s	144
$9a_1$	13.99	13.92	C2p, S3p, N2p	367
$7b_1$	13.79	13.81	C2p, N2p	157
$6b_2$	13.54	13.47	S3s,3p, C2p	347
$6a_2$	13.10	13.17	N2p, C2p	148
$7b_2$	12.99	12.86	S3p, N2p, C2p	332
$8b_1$	12.65	12.51	"π" C2p, N2p	322
$10a_1$	11.28	11.08	S3p, C2p, N2p	510
$8b_2$	10.07	9.65	S3p, N2p	827
$9b_1$	9.91	10.12	S3p, N2s, N2p	1186
$11a_1$	8.00	7.89	"π" S3p, N2p	906
$10b_1$	7.27	7.13	"π" N2p	218
$7a_2$	7.12	7.33	N2p, S3p	788
$9b_2$	6.85	7.21	"π" N2s,2p	473
$12a_1$	6.62	6.67	"π" S3p, N2p	783
$8a_2$ (HOMO)	−6.16	−5.80	"π" N2p	234
$10b_2$ (LUMO)	+3.29	+4.18	σ S3p	

Table IV. Core-Peak Binding Energies of DTZ and DIATZ[a]

	DTZ	DIATZ
C1s E_b	284.4-286.6	285.1-287.3 (284.0)[b]
fwhm	1.1 1.0	1.7 1.3
satellites position (relative to the main peak)	290.3 (3.7)	
N1s E_b	398.7	397.7-399.4
l |n| n |n| n		
fwhm	1.0	2.9
satellites position (relative to the main peak)	403.0 (4.3)	
$S2p_{3/2}$ E_b	165.4	165.5 (164.0)[a]
l |n| n |n| n		
$fwhm_{tot}$	2.0	2.5
satellites position (relative to the main peak)	169.1 (3.7)	171.3 (5.8)

[a] (E_b = binding energy; fwhm = full-width at half-maximum) (eV). [b] Binding energies in parentheses refer to impurities.

Table V. Valence-Peak Binding Energies of DTZ and DIATZ (eV)[a]

	DTZ	DIATZ
A	21.8	22.6
B	20.0	
C	17.0	16.9
D	13.3	14.5
E	9.6	10.1
F	6.8	6.6-5.5
G	4.4	3.5
H	2.3	?

[a] Labels refer to Figure 5.

binding energy as the HOMO in DTZ, namely around 2.3 eV, but with a much lower intensity than the neighboring occupied MO (Table III). Therefore, the HOMO is probably located on the right hand side of peak G and is hidden by the overlapping of more intense MO's located around 3.4 eV.

C. Core Level Satellites. The C1s core peaks of DTZ are accompanied by a broad satellite centered around 290.3 eV, appearing 5.9 eV on the left hand side of the C1s line of the phenyl carbons and at 3.7 eV from the C1s line of the endocyclic carbon atoms. Another satellite is observed at the same energy separation, 3.7 eV, on the left hand side of the S2p line (Table IV). We therefore think that these two satellites are related to the same $\pi \rightarrow \pi^*$ shake-up transition. Their presence in the vicinity of the

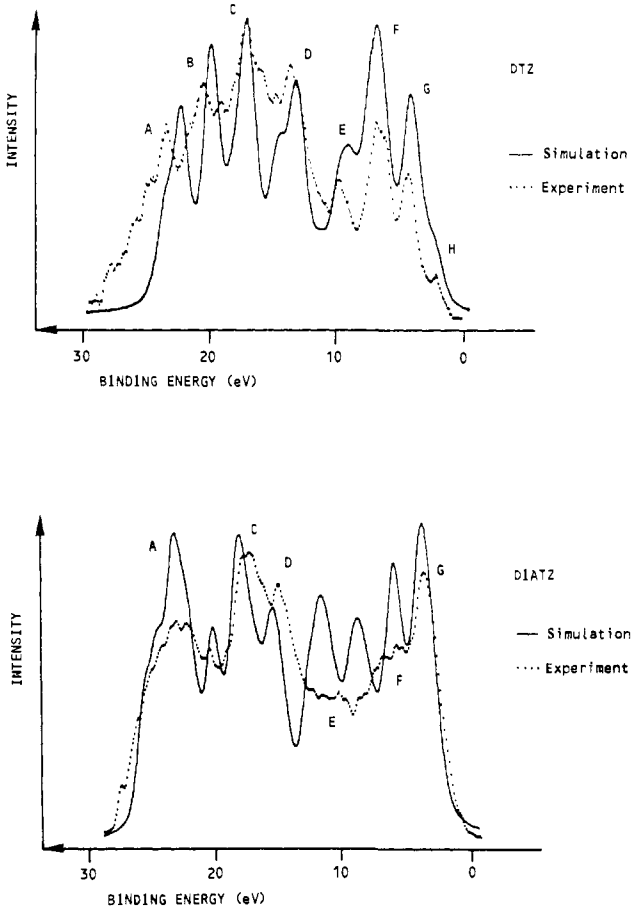

Figure 6. Experimental and simulated valence-band spectra of DTZ and DIATZ.

C1s and S2p lines and their absence in the neighborhood of the N1s core level, combined with the rather low amplitude (at 3.7 eV) of the transition, may suggest that the transition has its origin in the HOMO, which exhibits significant electron densities on the S_1 and C_3 atoms. The broadness of the satellite line at 290.3 eV is probably due to the simultaneous existence of the well-known[18] $\pi \rightarrow \pi^*$ shake-up of the phenyl rings occuring in the same energy range, i.e., at 5.9 eV from the main C1s line.

The N1s level is also followed by a satellite at 403.0 eV, 4.3 eV higher in binding energy than the main peak. From the MO diagram in Figure 2, this shake-up process could originate from the π $2a_{1u}$ level. The absence of such a feature in the vicinity of the C1s and S2p peaks agrees with the electron density map of this π orbital.

In the case of DIATZ we only observe structure at 5.8 eV after the S_{2p} peak, but the impurities detected in the spectrum do not allow the assignment of this feature to a shake-up transition involving an MO of DIATZ.

Concluding Remarks

The electronic structure of diphenyl- and bis(dimethylamino)dithiatetrazocines as revealed by XPS and ab initio results shed some light on the origin of the conformational differences exhibited by two closely related compounds. The dithiatetrazocine heterocycle alone obeys the $4n + 2$ Hückel rule and per se should be planar. Strong electron donor groups increase the electron density on the $S_2N_4C_2$ framework, thereby inducing structural stresses and a destabilization of the heterocycle. As a consequence, the geometry of the whole molecule changes by developing a bonding interaction between the ring sulfurs, in order to lower the total energy at the price of a loss in the aromatic character.

Participation of the S3d orbitals must be discussed with caution. It is indeed difficult to estimate their involvement in the regulation of the structures. In each compound, they induce a significant reduction of the S-N bond polarity. They seem, however, to play a minor role in the shape of the occupied molecular orbitals. Their somewhat more pronounced participation in the unoccupied MO's suggests a more active contribution in properties related to excited states.

Registry No. DTZ, 76843-75-9; DIATZ, 76843-76-0.

(18) Nordberg, R.; Albridge, R. G.; Bergmark, T.; Ericson U.; Hedman, J.; Nordling, C.; Siegbahn, K.; Lindberg, B. J. *Ark. Kemi* **1968**, *28*, 257.
(19) Riga, J.; Pireaux, J. J.; Verbist, J. J. *Mol. Phys.* **1977**, *34*, 131.

Mechanism of Phosphine Photolysis. Application to Jovian Atmospheric Photochemistry

J. P. Ferris,* Alain Bossard, and Haider Khwaja

Contribution from the Department of Chemistry, Rensselaer Polytechnic Institute, Troy, New York 12181. *Received October 8, 1982*

Abstract: PH_3 is photolyzed to H_2 and P_2H_4 and the P_2H_4 in turn is converted to red phosphorus. The initial quantum yield of H_2 formation was redetermined and found to be 0.93 ± 0.07. Red phosphorus was identified by its chemical properties and by the absence of P-H stretching bands in its infrared spectrum. The reaction pathway was not changed by lowering the PH_3 partial pressure from 90 to 11 torr or by performing the photolysis in a 70-fold excess of H_2. The initial quantum yields at 11 torr of PH_3 are $\Phi_{P_2H_4} = 0.40 \pm 0.02$ and $\Phi_{H_2} = 0.74 \pm 0.08$. The initial rate of P_2H_4 formation was not affected by lowering the PH_3 temperature to 227 or 157 K. The yield was greater at 157 K because the P_2H_4 condensed and was protected from further destruction. The initial quantum yields for the formation of P_2H_4 and H_2 in PH_3-NH_3 mixtures were comparable to those observed for PH_3 alone. Photolysis of mixtures in which NH_3 was absorbing 90% of the light resulted in the rapid formation of P_2H_4. No N_2 was formed when PH_3-NH_3 mixtures were photolyzed, suggesting that the destruction of NH_3 is quenched by PH_3. The application of these findings to Jovian atmospheric chemistry is discussed.

Our initial studies on the mechanism of phosphine (PH_3) photolysis with a 206.2-nm light established that diphosphine (P_2H_4) was the initial stable photoproduct and intermediate in the formation of red phosphorus.[1,2] Comparable findings for 147-nm light sources were reported subsequently.[3,4] It has been proposed that the color of the Great Red Spot on Jupiter is due

(1) Ferris, J. P.; Benson, R. *Nature* (London) **1980**, *285*, 156-157.
(2) Ferris, J. P.; Benson, R. *J. Am. Chem. Soc.* **1981**, *103*, 1922-1927.
(3) Blazejowski, J.; Lampe, F. W. *J. Phys. Chem.* **1981**, *85*, 1856-1864.
(4) Blazejowski, J.; Lampe, F. W. *J. Photochem.* **1981**, *16*, 105-120.

0002-7863/84/1506-0318$01.50/0